Atmospheric
Measurement
Techniques
Open Access
Discussions

Reporting the sensitivity of Laser Induced Fluorescence instruments used for HO$_2$ detection to an interference from RO$_2$ radicals and introducing a novel approach that enables HO$_2$ and certain RO$_2$ types to be selectively measured

L. K. Whalley[1,2], M. A. Blitz[1,2], M. Desservettaz[1], P. W. Seakins[1,2], and D. E. Heard[1,2]

[1]School of Chemistry, University of Leeds, Leeds, LS2 9JT, UK
[2]National Centre for Atmospheric Science, University of Leeds, Leeds, LS2 9JT, UK

Correspondence to: L. K. Whalley (lisakw@chem.leeds.ac.uk)

AMTD

6, 6249–6292, 2013

Sensitivity of Laser Induced Fluorescence instruments

L. K. Whalley et al.

Title Page

Abstract	Introduction
Conclusions	References
Tables	Figures

◄◄	►►
◄	►
Back	Close

Full Screen / Esc

Printer-friendly Version

Interactive Discussion

Abstract

Laboratory studies have revealed that alkene-derived RO_2 and longer-chain alkane-derived RO_2 ($> C_3$) radicals rapidly convert to HO_2 and then to OH in the presence of NO in a Fluorescence Assay by Gas Expansion (FAGE) detection cell (Fuchs et al., 2011). Three different FAGE cells that have been used to make ambient measurements of OH and HO_2 in the University of Leeds ground-based instrument have been assessed to determine the sensitivity of each cell, when operating in HO_2 detection mode, to RO_2 radicals. The sensitivity to this interference was found to be highly dependent on cell design and operating parameters. Under the operating conditions employed during fieldwork undertaken in the Borneo rainforest in 2008, an OH yield of 17 % was experimentally determined for both ethene- and isoprene-derived RO_2 radicals. The high pumping capacity of this system, resulting in a short residence time, coupled with poor mixing of NO into the ambient air-stream for the titration of HO_2 to OH effectively minimised this potential interference. An OH yield of 46 % was observed for ethene-derived RO_2 radicals when a smaller detection cell was used, in which the mixing of NO into the ambient air was improved and the cell residence times were longer. For a newly developed RO_x LIF cell, used for detection of HO_2 and RO_2 radicals, when running in HO_x mode an OH yield of 95 % was observed for ethene-derived RO_2 radicals.

In experiments in which conditions ensured the conversion of RO_2 to OH was complete, the yields of OH from a range of different RO_2 species agreed well with model predictions based on the Master Chemical Mechanism version 3.2. For ethene and isoprene derived RO_2 species, the relative sensitivity of FAGE was found to be close to that for HO_2 with an OH yield of 100 % and 92 % respectively. For the longer-chain alkane-derived RO_2 radicals, model predicted OH yields were highly dependent upon temperature. A model predicted OH yield of 74 % at 298 K and 36 % at 255 K were calculated for cyclohexane derived RO_2 radicals and an experimental yield of 38 % was

Sensitivity of Laser Induced Fluorescence instruments

L. K. Whalley et al.

Title Page

Abstract	Introduction
Conclusions	References
Tables	Figures

◄◄ ►►

◄ ►

Back Close

Full Screen / Esc

Printer-friendly Version

Interactive Discussion

observed indicating that the temperature within the cell was below ambient owing to the supersonic expansion of the airstream in the low pressure cell.

These findings suggest that observations of HO_2 by some LIF instruments worldwide may be higher than the true value if the instruments were sensitive to these RO_2 species. If this is the case, it becomes necessary to compare atmospheric chemistry model simulations to HO_2^* observations, where $HO_2^* = [HO_2] + \alpha\,[RO_2]$ and α is the mean fractional contribution of the RO_2 species that interfere (RO_2i). This methodology, however, relies on model simulations of speciated RO_2 radicals, as instrumentation to make speciated RO_2 measurements does not currently exist. Here we present an approach that enables the concentration of HO_2 and RO_2i to be selectively determined by varying the concentration of NO injected into a FAGE cell. Measurements of $[HO_2]$ and $[RO_2i]$ taken in London are presented.

1 Introduction

OH and HO_2 radicals, collectively termed HO_x, together with RO_2 radicals, control the oxidative chemistry in the atmosphere, being responsible for the transformation of primary emissions into secondary pollutants such as NO_2, O_3 and particulates. OH radicals control the lifetime of some greenhouse gases (e.g. CH_4), the production of acidic species (e.g. H_2SO_4) and aerosol precursors such as oxygenated volatile organic compounds. Understanding the behaviour of free-radicals in the atmosphere is of paramount importance in understanding the lifetimes of pollutants and hence the spatial scales of their transport. Predictive models for future air quality and climate change contain complex chemical schemes, and comparison with measurements of free-radicals (the concentrations of which are controlled only by local chemistry and not by transport) in the present atmosphere constitutes one of the best validations of these schemes (Heard and Pilling, 2003). OH and HO_2 radicals in the troposphere have been measured since the early 1990s using laser induced fluorescence (LIF) spectroscopy at low pressure (Fluorescence Assay by Gas Expansion, or the FAGE technique) orig-

inally developed by Hard et al. (1979, 1984). The technique employs 308 nm radiation, produced using a variety of laser technologies, to excite OH radicals, which fluoresce; this emission (also at 308 nm) is detected and used to quantify OH. It is also possible to simultaneously detect HO_2 in a second fluorescence cell, by chemical conversion to

5   OH through reaction with NO and subsequent detection by LIF. The technique has been employed by several groups worldwide for the detection of OH and HO_2 (Hofzumahaus et al., 1996; Mather et al., 1997; Kanaya et al., 1999; Creasey et al., 2001; Faloona et al., 2001; Hanisco et al., 2002; Holland et al., 2003; Heard and Pilling, 2003; Stone et al., 2012). Specific to this work, the Leeds ground-based FAGE instrument has been

10   operational since 1996 and has detected OH and HO_2 under a variety of conditions ranging from urban (Heard et al., 2004) to clean marine (Whalley et al., 2010). Although the FAGE technique represents an extremely sensitive (typical OH detection limits are in the low to mid 10^5 molecule cm^{-3}) (Heard and Pilling, 2003) and selective method for OH and HO_2 detection, ambient HO_x concentrations are themselves

15   extremely low (OH concentrations are typically a few 10^6 molecule cm^{-3}) (Stone et al., 2012), thus, care needs to be taken to ensure that any measurement is not biased by any chemical or spectral interference.

A well-documented example of an OH interference comes from the earliest tropospheric LIF instruments (Davis et al., 1981; Ortgies et al., 1980; Shirinzadeh et al.,

20   1987), which used off-resonant pulsed laser excitation of the OH radical at 282 nm, via the $A^2\Sigma^+(\upsilon' = 1) \leftarrow X^2\Pi_i(\upsilon'' = 0)$ transition. These instruments were found to suffer from a considerable interference from laser-generated OH formed by the laser photolysis of ambient ozone and subsequent reaction of $O(^1D)$ with ambient water vapour:

$$O_3 \xrightarrow{h\nu} O(^1D) + O_2 \tag{R1}$$

25   $$O(^1D) + H_2O \rightarrow 2OH \tag{R2}$$

The use of OH detection at lower pressure (reducing $[H_2O]$ and hence the rate of R2), lower laser energy per pulse (the OH artefact signal depends on the square of the laser energy) and switching to excitation at 308 nm (the H_2O/O_3 interference is
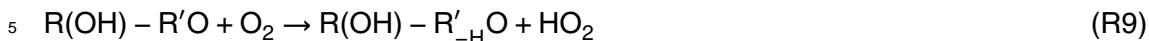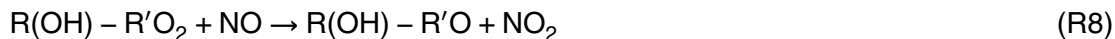
30 times lower than at 282 nm) almost completely overcame this problem. Holland et al. (2003), however, observed an interference in the presence of ozone and water vapour that appeared to be a dark reaction on the walls of their detection cell which produced a source of HO_2 radicals; the authors report a signal equivalent to 5.4×10^7 molecule cm^{-3} of HO_2 in the presence of 50 ppbv O_3 and at a relative humidity of 60 %. This interference has been characterised in detail and is subtracted from their ambient HO_2 measurements.

In the presence of the added NO used to convert HO_2 to OH inside the fluorescence cell, and hence enable HO_2 to be measured, organic peroxy radicals (RO_2) also have the potential to be chemically converted to OH via:

$$RO_2 + NO \rightarrow RO + NO_2 \tag{R3}$$
$$RO + O_2 \rightarrow HO_2 + R_{-H}O \tag{R4}$$
$$HO_2 + NO \rightarrow OH + NO_2 \tag{R5}$$

Due to the low pressure employed in FAGE detection, however, R4 is slow ($\sim 12\,s^{-1}$ for CH_3O at 1 Torr) and, given the very short residence time in FAGE between NO injection and the detection region of typically just a few milliseconds (Creasey et al., 1997b), it was assumed, until recently, that RO_2 radicals were not converted to OH to any large extent. In support of this, Ren et al. (2004) reported no interference upon introduction of C_1–C_4 alkane derived RO_2 radicals in the Penn. State FAGE system, and concluded that there was no evidence of any significant interferences for OH or HO_2 measurements in the atmosphere, including in highly polluted urban environments. Only recently has an interference from alkene and aromatic derived RO_2 species been reported (Fuchs et al., 2011). Unlike alkane-derived RO_2 species which are formed via H-atom abstraction from the parent alkane and subsequent addition of O_2 (Reaction R6), the major pathway to alkene-derived RO_2 formation is via OH addition across

the double bond followed by O_2 addition (Reaction R7):

$$RH + OH \xrightarrow{O_2} RO_2 + H_2O \tag{R6}$$

$$R = R' + OH \xrightarrow{O_2} R(OH) - R'O_2 \tag{R7}$$

$$R(OH) - R'O_2 + NO \rightarrow R(OH) - R'O + NO_2 \tag{R8}$$

$$R(OH) - R'O + O_2 \rightarrow R(OH) - R'_{-H}O + HO_2 \tag{R9}$$

$$R(OH) - R'O \xrightarrow{Decomp.} R{=}O + R'{-}OH \tag{R10}$$

$$R' - OH + O_2 \rightarrow R{=}O + HO_2 \tag{R11}$$

The β-hydroxyalkylperoxy radical formed reacts with NO to form a β-hydroxyalkoxy radical (Reaction R8) which can either react with O_2 (Reaction R9) or decompose to a hydroxyalkyl radical (Reaction R10) which then reacts rapidly with O_2 to form a carbonyl and HO_2 (Reaction R11). Compared to the slow $RO + O_2$ reaction ($k = 1.65 \times 10^{-15}\,cm^3\,molecule^{-1}\,s^{-1}$, for $R = CH_3$, (Reaction R9), Orlando et al., 2003), decomposition and subsequent reaction of the hydroxyalkyl radical (CH_2OH) with O_2 is fast ($k = 9.6 \times 10^{-12}\,cm^3\,molecule^{-1}\,s^{-1}$, Atkinson et al., 1997). Fuchs et al. (2011) found, due to this rapid decomposition pathway, that RO_2 species formed from alkene and aromatic precursors were detected as OH with relative sensitivities greater than 80 % with respect to that for detection of HO_2 in their FAGE system. The level of the interference was found to be highly dependent upon the NO concentration injected and reaction time between injection and OH detection, which was varied by Fuchs et al. (2011) suggesting that other FAGE instruments with different cell designs and operational parameters may display different sensitivities towards this interference. FAGE cells used for airborne HO_2 measurements tend to have longer inlets to extend through the fuselage of the aircraft and, hence, sampled air tends to have longer residence times in these cell types compared to cells used solely for ground measurements. Very recently, Mao et al. (2012) reported an average RO_2 sensitivity of ~ 60 % with respect to that for HO_2 for a selection of alkene-derived RO_2 species in the Penn.

Sensitivity of Laser Induced Fluorescence instruments

L. K. Whalley et al.

State FAGE instrument, whilst Vaughan et al. (2012) reported a sensitivity to ethene-derived RO_2 radicals of 40 % with respect to that for HO_2 for the University of Leeds aircraft FAGE instrument (Commane et al., 2010). Ultimately the measurement bias on the HO_2 concentrations reported from past field studies will depend upon the indi-
5 vidual FAGE instruments utilised (because of variations in key operating parameters such as residence time) and the concentration and speciation of RO_2 present. Many FAGE groups now report HO_2^* for comparison with atmospheric chemistry box models (Lu et al., 2012) where $HO_2^* = [HO_2] + \alpha [RO_2]$, and α is the mean fractional contribu-tion of the RO_2 species that interfere (RO_2i) in a particular instrument which has been
10 determined experimentally.

  Together with an HO_2 interference, FAGE measurements of OH are reported to have an interference for one instrument type in forested environments (Mao et al., 2012). The authors postulate that OH may be generated in their FAGE cell in the presence of ozone and alkenes with laser-generated OH within the cell being ruled out. Similar to
15 the HO_2 interference reported here, this OH interference may be dependent upon the particular design of this FAGE cell, for example the residence time between sampling and detection and, as such, the extent that other OH measurements suffer from this interference is unknown, meaning that it is critical that a set of standardised experi-ments are performed on different FAGE cell types used for ambient detection of OH
20 to assess the extent of any interference. Good agreement between two independent OH measurements made using Differential Optical Absorption Spectroscopy (DOAS) and LIF was observed during a series of experiments performed in the SAPHIR at-mospheric simulation chamber under a range of atmospheric conditions (Fuchs et al., 2012) suggesting that the Julich FAGE system, at least, does not suffer an interference
25 when detecting OH under the conditions studied.

  In this paper we report results from interference studies performed using the Uni-versity of Leeds ground-based FAGE instrument (Creasey et al., 1997a) measuring in HO_2 mode (NO added to the detection cell) and discuss the likely impact of the RO_2 interference on previous field studies. We also compare absolute yields of OH from

Title Page

Abstract | Introduction

Conclusions | References

Tables | Figures

|◄ | ►|

◄ | ►

Back | Close

Full Screen / Esc

Printer-friendly Version

Interactive Discussion

alkene-derived and higher alkane-derived RO_2 species in the presence of NO where conditions allowed reactions to proceed to completion and compare with MCMv3.2 recommendations.

2 Experimental

HO_2 and RO_2 radicals were generated prior to FAGE detection by two different methods: a steady-state turbulent flow tube reactor calibrated for absolute radical concentrations and a time-resolved laser flash photolysis system. Each method will be described in turn.

2.1 Steady state experiments

The FAGE calibration system (described in detail by Commane et al., 2010) acts as a turbulent flow reactor and generates known and equal quantities of OH and HO_2 radicals by the 184.9 nm photolysis of H_2O vapour by a Hg penray lamp in a humidified air stream (Reactions R12 and R13):

$$H_2O + hv \rightarrow H + OH \tag{R12}$$

$$H + O_2 \xrightarrow{M} HO_2 \tag{R13}$$

With knowledge of the product of the lamp flux and irradiation exposure time past the lamp (determined by N_2O actinometry, Commane et al., 2010) the concentration of OH and HO_2 may be determined; typical radical concentrations generated by this method range from $< 10^7$–10^9 molecule cm^{-3}. RO_2 radicals (in the presence of HO_2 from R13) were generated by introducing the parent hydrocarbon into the FAGE calibration system approximately 2.5 cm after the penray lamp. The OH generated in the calibration photolysis region reacted rapidly with the hydrocarbon introduced, Reaction (R6), generating RO_2 radicals. To assess the magnitude of any HO_2 interference suffered during previous ambient field measurements, a number of individual peroxy

radical species were generated and introduced into three different fluorescence cells (Fig. 1) which have been used during field deployments by the Leeds group (further details on the fieldwork FAGE detection cells tested are given below). The peroxy radicals tested were derived from methane, propane, ethene, isoprene, toluene, cyclohexane and methanol. A small flow ($\sim$ 10–150 Standard Cubic Centimetre per Minute, SCCM) of a dilute (0.1–5 %) hydrocarbon mix in N_2 (ethene, isoprene, toluene, cyclohexane or methanol) or a 100 % hydrocarbon flow of propane (10 SCCM) or methane (500 SCCM) was introduced into a 20–40 Standard Litre per Minute (SLM) humidified airstream approximately 5 cm before the exit of the calibration tube. The residence time within the calibration flow tube ($\sim$ 10 ms at 40 SLM) was sufficient to ensure complete conversion of OH to RO_2 before being sampled in the fluorescence cells. In the case of ethene, at an initial concentration of 3.1×10^{14} molecule cm^{-3}, it takes $\sim$ 1 ms for complete conversion of OH to RO_2, using a rate coefficient, $k_{C_2H_4+OH}$, equal to 2.86×10^{-11} molecule^{-1} cm^3 s^{-1} (Cleary et al., 2006). This could be experimentally verified by observing the complete loss of the OH signal upon addition of the hydrocarbons when no NO was added to the FAGE expansion cells; this complete loss of OH signal was observed even for the slowest reacting hydrocarbon species (e.g. methane).

FAGE detection cells

The University of Leeds ground-based FAGE instrument described in detail elsewhere (Whalley et al., 2010) was assessed to determine the magnitude of the HO_2 interference from selected RO_2 species under configurations employed in two recent field studies. The first, the Oxidants and Particle Photochemical Processes (OP3) (Hewitt et al., 2010) which took place in the Borneo rainforest (Whalley et al., 2011) and the second, the Hill Cap Cloud Thuringer – 2010 (HCCT-2010) (Whalley et al., 2013) which aimed to quantify the loss of radicals to cloud droplets.

The operational parameters of the different FAGE fluorescence cells considered are quite different and are summarised in Table 1. During OP3, one 22 cm internal diame-

ter cylindrical, stainless steel fluorescence cell was used to make sequential measurements of OH and HO_2 (Fig. 1a). Air was drawn into the cell via a 5 cm tall, 2.54 cm diameter turret through a 1 mm diameter pinhole nozzle in a flat plate (0.1 mm thickness). The cell was maintained at approximately 0.9 Torr using a Roots blower backed

5 by a rotary pump (Leybold)). The cell was connected to the pump system via a 10 cm ID, 5 m length stainless steel flexible hose. NO was injected into the cell 7.5 cm below the nozzle via a custom-built injection ring containing four injection points, spaced 4 cm apart, and made from 1.6 mm (ID) tubing in a square arrangement located around the air stream. 50 SCCM NO was injected into the cell via a computer-controlled solenoid

10 valve (Metron Semiconductors) and calibrated mass flow controller (MKS 1179A, range 0–50 SCCM) during the second half of the collection period when the laser was tuned to the OH transition. As only one cell was used for sequential detection of OH and HO_2, the conditions were optimised to maximise the sensitivity towards OH. Under these conditions the conversion of HO_2 to OH was only $\sim 10\%$, most likely due to poor mixing

15 of the NO into the ambient air flow caused by the particular flow characteristics created by the combination of the 1 mm diameter pinhole nozzle and the pressure and pumping speeds employed. The 10 % conversion of HO_2 to OH determined assumes that there is no preferential loss of either radical in the calibration system, i.e. that the concentration of OH and HO_2 are equal as they enter the FAGE detection cell. This assumption

20 has previously been verified by addition of sufficient CO to the calibration system so as to rapidly convert all the OH to HO_2 (Reaction R14) and the HO_2 signal was observed to double in the presence of CO. The radicals sampled, or converted from HO_2, were electronically excited at 308 nm, approximately 13 cm below the sampling nozzle using a tuneable, 5 KHz pulse repetition frequency laser (Nd : YAG pumped Ti : Sapphire,

25 Photonics Industries) with the fluorescence at the same wavelength detected perpendicular to the laser axis by a filtered (Barr Associates filter, transmission > 50 % at 308 nm) channel photo-multiplier, CPM, (Perkin Elmer) and gated-photon counting.

During the HCCT-2010 campaign one FAGE fluorescence cell was also used to measure both radical species. The cell was operated from the top of a 22 m high tower to

Title Page

Abstract | Introduction

Conclusions | References

Tables | Figures

◄ | ►|

◄ | ►

Back | Close

Full Screen / Esc

Printer-friendly Version

Interactive Discussion

co-locate with hill-cap cloud measurements and ensure that the radical measurements were performed in full cloud. As a result of these requirements a smaller cell, based on the University of Leeds aircraft FAGE fluorescence cell (Commane et al., 2010), was used to make sequential measurements of OH and HO_2 (Fig. 1b); operational details are provided in Table 1. NO (10 SCCM) was injected into this cell via 3.2 mm ID stainless tubing inserted into the centre of the ambient air stream. This configuration resulted in a high conversion of HO_2 to OH ($\sim 90\%$). Ambient air was drawn into the cell through a 1 mm diameter pinhole nozzle into a 4.5 cm (ID) stainless steel cylinder. The cell was held at 1 Torr and was connected to the roots-rotary pump system described above via 30 m of flexible hosing (5 cm ID). Laser light was delivered from the Nd : YAG pumped Ti : Sapphire laser system to the cell via a 30 m fibre optic. The distance between sampling nozzle and detection was 18 cm with the NO injected ~ 8 cm below the nozzle.

The third FAGE cell tested for an RO_2 interference was a recently developed fluorescence cell designed for the detection of RO_2 radicals, alongside OH and HO_2, using the "RO_xLIF" methodology outlined by Fuchs et al. (2008). The RO_2 cell is operated in two modes, providing a measurement of the sum of OH + HO_2 in HO_x mode and the sum of OH + HO_2 + RO_2 in RO_x mode. Experiments were run on this third FAGE cell to determine the magnitude of the HO_2 interference suffered from a variety of RO_2 species in the HO_x mode.

A similar FAGE fluorescence cell as the one described above (Fig. 1a) was modified by coupling it to a differentially pumped reaction tube (held at approximately 30 Torr) to allow for conversion of RO_2 radicals to OH (Fig. 1c). The reaction tube is an 83 cm high, 6.4 cm diameter aluminium tube which has been coated with halocarbon wax to minimise radical wall losses. Ambient air (7.5 SLM) is drawn into the reaction tube through a 1 mm diameter pinhole drilled into a thin (1 mm thickness), flat plate aluminium inlet nozzle. In HO_x mode, 250 SCCM of CO (5 % in N_2, BOC) is flowed into the centre of the reaction tube just beneath the inlet (~ 2 cm below) via a 6.4 mm (ID) stainless steel tube. Hydroxyl radicals are converted to HO_2 by reaction with CO (Reaction R14) as

Title Page

Abstract | Introduction

Conclusions | References

Tables | Figures

◀ | ▶

◀ | ▶

Back | Close

Full Screen / Esc

Printer-friendly Version

Interactive Discussion

they pass through the reaction tube. Air ($\sim$ 5 SLM) from the reaction tube is sampled by the FAGE detection cell (held at approximately 1.5 Torr) via a 4 mm diameter pinhole nozzle sat on a 5 cm tall turret. Ambient HO_2 (and ambient OH which was converted to HO_2 in the reaction tube) is titrated to OH by NO injected into the cell 7.5 cm below the nozzle and detected by LIF; 100 SCCM of NO was injected into this fluorescence cell to maximise the conversion of HO_2 to OH. In RO_x mode, 25 SCCM of a 500 ppmv NO standard in N_2 (BOC) was added to the CO flow to promote conversion of RO_2 to OH (Reactions R3–R5); the excess CO present rapidly converts OH to HO_2 (Reaction R14) and helps to minimise the overall loss of the radicals to the walls of the reaction tube. Ambient RO_2, HO_2 and OH radicals (converted to HO_2 in the reaction tube) enter the FAGE detection cell, are reconverted to OH by NO and detected as described above.

$$OH + CO \xrightarrow{O_2} HO_2 + CO_2 \tag{R14}$$

2.2 Time-resolved experiments using laser flash photolysis

The time-resolved setup was based on a laser-induced pump and probe OH reactivity technique developed by Sadanaga et al. (2004) which uses pulsed 266 nm light to photolyse ozone in a flow tube to generate $O(^1D)$ and, by the subsequent reaction of $O(^1D)$ with H_2O vapour, OH radicals (Reaction R1–2). The flow tube used here was 173 cm in length with an internal diameter of 5 cm; a schematic of the experimental set-up is shown in Fig. 2. The total flow was typically 10 SLM and the pressure in the flow tube was 300 Torr, which was controlled by a valve throttling a rotary pump (Leybold). A FAGE cell was located approximately halfway along the flow tube, held perpendicular to the flow tube, and sampled the gas flow through a 1 mm diameter pinhole nozzle that was located within 1 cm of the central axis of the flow tube. A YAG laser (Spectron SL803) was used to generate $\sim$ 10 mJ pulse^{-1} of 266 nm photolysis radiation with a 10 ns pulse width; the beam profile was shaped using a Galilean telescope to produce a collimated beam with a diameter of $\sim$ 2 cm and directed along the flow tube

Title Page

Abstract | Introduction

Conclusions | References

Tables | Figures

◄ | ►►

◄ | ►

Back | Close

Full Screen / Esc

Printer-friendly Version

Interactive Discussion

such that the outer edge just illuminated the pinhole – gauged by the silhouette of the beam profile at the end of the tube.

The FAGE expansion cell was pumped by a rotary/roots blower pump combination (Leybold), which reduced the pressure in the expansion cell to 1 Torr, and typically sampled about 30 % of the total flow of the flow tube with the remaining flow evacuated from the flow tube via the rotary pump. The expansion cell was 4.5 cm in internal diameter with the fluorescence detection axis ∼ 23.5 cm from the pinhole. An excimer (Lambda Physik LPX105) pumped dye laser (Lambda Physik FL3002) operating on Rhodamine 6G generated visible light which was frequency doubled to 307.844 nm and used to probe the OH radical via the Q_1(1) (A-X) (0–0) transition; typical pulse energies and pulse lengths were 0.2 mJ pulse^{-1} and 20 ns respectively. The radiation was directed into the detection axis via a baffled entrance arm and the fluorescence was captured by a filtered (Barr Associates), gated CPM (Perkin Elmer) mounted at right-angles to the laser beam. The pump and probe lasers were typically operated with a pulse repetition frequency of 2.5 Hz.

A LabView™ program controlled the experiment via a GPIB interfaced to a delay generator (Berkley Nucleonics Corporation, BNC 555) and an oscilloscope (LeCroy LT264). The time between the photolysis and probe lasers was controlled by the delay generator, and OH time profiles were built-up by scanning the delay between the lasers over 200 points. At each time point the OH fluorescence signal was integrated across its entire decay on the oscilloscope before being transferred for storage on the computer.

Gases were introduced to the flow tube via mass flow controllers (MKS). Nitrogen (10 SLM), was passed through a water bubbler (HPLC grade) and then into a manifold to mix with oxygen (1 SLM), ozone (≤ 10 standard cubic centimetres – SCCM) and a reagent gas (≤ 40 SCCM), before admission into the flow tube. Ozone from an ozone generator (Easelec, ELO-3G) was used directly to fill a 5 L Pyrex bulb, and then pressurised with nitrogen (up to 2 bar) to give concentrations between 1–3 %. The reagent gases, methanol, n-butane, n-pentane, ethene, propene, isoprene and cyclohexane were degassed by freeze pump thawing, and known concentrations were prepared in

Title Page

Abstract | Introduction

Conclusions | References

Tables | Figures

|◄ | ►|

◄ | ►

Back | Close

Full Screen / Esc

Printer-friendly Version

Interactive Discussion

Pyrex 5 L bulbs. Pressure gauges (MKS) were used to determine the bulb concentrations and the pressure in the flow tube and FAGE cell.

The OH generated (approximately 10^{10} molecule cm^{-3}) via the photolysis of ozone in the presence of H_2O vapour (Reactions R1–2) reacted rapidly with the added reagents in the presence of O_2 forming peroxy radicals (Reaction R6) or in the case of methanol, HO_2 formed via the following reactions:

$$OH + CH_3OH \rightarrow CH_2OH + H_2O \tag{R15}$$
$$CH_2OH + O_2 \rightarrow HO_2 + CH_2O \tag{R16}$$

or

$$OH + CH_3OH \rightarrow CH_3O + H_2O \tag{R17}$$
$$CH_3O + O_2 \rightarrow HO_2 + CH_2O \tag{R18}$$
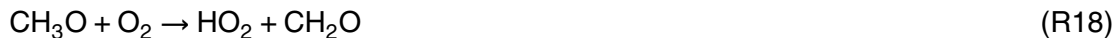
OH reacts with methanol, predominantly forming CH_2OH (reported yields of 0.75–0.85, Atkinson et al., 2004) (Reaction R15) which then rapidly reacts with O_2 (9.6 × 10^{-12} cm^3 molecule^{-1} s^{-1}) (Atkinson et al., 2004) to form HO_2 (Reaction R16). The other, minor, abstraction channel produces CH_3O, which reacts slower with O_2 (1.92 × 10^{-15} cm^3 molecule^{-1} s^{-1}) (Atkinson et al., 2004) to produce HO_2 (Reaction R17, 18). HO_2 generated in the system was detected by adding nitric oxide (NO – 99.95 %, BOC) to the FAGE expansion cell (Fig. 2) to titrate to OH for subsequent detection (Reaction R5). The NO flow, controlled by a mass flow controller (Brookes) (0–50 SCCM), was injected into the centre of the FAGE cell, via 3.2 mm stainless steel tubing, approximately 13.75 cm below the pinhole. The fluorescence signal observed when NO is added to the expansion cell derives from OH and converted HO_2 (OH + αHO_2), where α is equal to the titration efficiency of Reaction (R5), which is a function of the amount of NO added and the contact time in the expansion cell. For complete conversion of HO_2 to OH in the detection cell α will equal 1. If this is the case, in the presence and absence of methanol there should be no overall change in the initial fluorescence signal when NO was added as the OH lost in Reaction (R15) is rapidly converted to HO_2

in Reaction (R16) and then back to OH via reaction with NO. In the time-resolved experiments, a 6 SCCM flow of NO was found to provide the maximum conversion of HO_2 to OH (close to 100 %).

2.3 Model comparison

The measured HO_2 yields from the different RO_2 species studied have been compared with model predictions based on the Master Chemical Mechanism (MCM) version 3.2 (http://mcm.leeds.ac.uk/MCM/home.htt) (Jenkin et al., 1997; Carslaw et al., 1999b; Saunders et al., 2003; Jenkin et al., 2003; Bloss et al., 2005). The chemical reactions which convert the various VOC tested to OH that were incorporated in the model are listed explicitly in the Supplement (SI). The MCM makes the assumption that alkoxy radicals either react with O_2 to form a carbonyl species and HO_2 or decompose (or in the case of the $> C_3$ alkane-derived alkoxy radicals, isomerise) to form a hydroxyalkyl radical. Within a low temperature FAGE expansion, however, in the presence of NO, the reaction of alkoxy radicals and NO may begin to compete as the rate of decomposition and isomerisation slows considerably at reduced temperatures (as discussed further in Sect. 4, temperatures may drop as low as 25 K within the jet and remain below ambient temperatures in the region between NO injection and detection (Creasey et al., 1997b)). To account for this, (Reaction R19) has been included in model predictions with all rate coefficients for the reaction of various RO radicals with NO taken from the review paper by Heicklen (2007).

$$RO + NO \xrightarrow{M} RONO \tag{R19}$$

For reactions between alkoxy radicals and NO which do not have reported rate coefficients, $k_{RO+NO} = 3.3 \times 10^{-11} \, cm^3 \, molecule^{-1} \, s^{-1}$, (average rate coefficient for reaction of C_3–C_5 RO radicals with NO) was assumed. The model was initialised with the radical concentrations used and [NO] and [O_2] which encompassed experimental conditions within the FAGE expansion cell. The concentrations of all other intermediate species or products were initialised as zero. [NO] was varied between 1×10^{13}–

1×10^{14} molecule cm^{-3} depending upon the NO flow rates introduced to each of the FAGE detection cells. For the large FAGE detection cells (of the style cell A or C), good agreement between the model and experiment is only achieved if the concentration of NO in the jet is lower than that calculated from the initial NO injection flow rate suggesting that the mixing within the jet is poor for these cells (see Sect. 4.2 for further details). The simultaneous rate equations were solved using an Excel based integrator, Kintecus (Ianni, 2002). The model runs were 80 ms in duration, which provided sufficient time for complete conversion of peroxy radicals to OH under the time-resolved experimental conditions discussed above.

3   Results

3.1   RO$_2$ interferences in HO$_2$ measurements using fieldwork FAGE instrumentation

A variety of RO$_2$ species were generated in the turbulent flow reactor and introduced into the three FAGE cells, A–C (Fig. 1) described in Sect. 2.1. The yield of OH from the different RO$_2$ species for the different cells is given in Table 1. The flow reactor produces OH and HO$_2$ in equal quantities in the absence of a hydrocarbon (Fuchs et al., 2011). Upon addition of a hydrocarbon all the OH generated is quickly consumed (on a timescale of the order of 1×10^{-4} s) and RO$_2$ radicals form. In the case of propane or methane, the RO$_2$ formed does not yield appreciable OH (via the formation of HO$_2$) in the FAGE expansion cells in the presence of NO (as shown by the time-resolved experiments, Sect. 3.2, the OH yield from propane was < 4 %), and so any fluorescence signal observed upon NO addition relates solely to the co-generated HO$_2$. The yield of OH from RO$_2$i species can be determined by comparing the fluorescence signal observed when a RO$_2$i species was present (HO$_x$ signal$_{(reagent)}$) with the OH yield from HO$_2$ alone (HO$_2$ signal in the propane or methane experiments, which have no

interference) using Eq. (1):

$$\text{Relative OH yield} = \frac{HO_x signal_{(reagent)} - HO_2\ signal}{HO_2\ signal} \qquad (1)$$

The flows of hydrocarbons were adjusted so that equivalent OH reactivities (k_{HC+OH}[HC]) for each of the hydrocarbons tested were used to ensure that any other loss of OH in the turbulent flow reactor (e.g. loss to walls) did not bias the relative yields determined.

In a number of experiments the NO concentration added to detection cell A was varied and the ratio of the OH signal observed for propane-derived RO_2 radicals relative to ethene-derived RO_2 radicals were compared and are shown in Table 1 and Fig. 6. As the NO concentration was reduced the interference from alkene-derived RO_2 radicals decreased. By varying [NO], it becomes possible to discriminate ambient RO_2 radicals from ambient HO_2 radicals and this is discussed further in Sect. 4.2.

3.2 Time-resolved experiments

To determine the absolute yield of OH from different RO_2 radicals in the presence of NO, a range of RO_2 radicals (or HO_2 in the case of methanol) were generated by the addition of different parent hydrocarbons to the flow tube described in Sect. 2.2 coupled to a FAGE cell in which there was sufficient time for complete conversion of RO_2 to OH. The time-resolved OH signals observed for a selection of RO_2 species tested are shown in Fig. 3, and Table 2 summarises the OH yields for all RO_2 investigated.

As the initial OH concentration generated and subsequent HO_2 or RO_2 concentration generated within the flow tube were uncalibrated, the absolute OH yields within the FAGE expansion cell from the different RO_2 species were determined by comparing with the OH signal observed from HO_2 generated in the methanol experiments which has a 100 % yield. An exponential function of the form: $y = y_0 + A \times \exp(-B \times x)$ was fitted to each OH temporal profile associated with the different RO_2 species investigated. To

determine the relative yields of OH, the ratio of the *A* factor for each fit relative to the *A* factor determined for the methanol fit was calculated using Eq. (2):

$$\text{Relative OH yield} = A \text{ factor}_{(reagent)} : A \text{ factor}_{(methanol)} \tag{2}$$

In agreement with Fuchs et al. (2011), a large OH yield from alkene-derived RO_2 radi-
cals was observed (see Table 2) when NO was present in the FAGE cell. Smaller, but still significant, OH yields were also observed for RO_2 radicals derived from cyclohex-ane, *n*-butane and *n*-pentane (Table 2); the OH signal observed for propane-derived RO_2 radicals was negligible (upper limit of 4 %).

In several experiments, it was found that ethene and propene-derived RO_2 radicals when compared to HO_2 from methanol had OH yields greater than one. The formation of β hydroxy peroxy radicals is fast in the flow tube, and, if complete RO_2 titration to HO_2 and ultimately to OH is occurring in the FAGE cell then the ratio of the OH signals observed in the presence of ethene, propene and methanol is expected to equal one. A value greater than one suggests incomplete conversion of methanol to HO_2 in the flow tube. It was observed in experiments where the Pyrex bulb containing methanol was left for a full day before use to allow for mixing (such an experiment is displayed in Fig. 3) rather than just a couple of hours, that yields close to one were obtained indicating that in several of the experiments there may have been insufficient methanol reaching the flow tube owing to extremely slow mixing of the gas bulb. To ensure that the results are not biased by a possible problem with methanol, the third column in Table 2 shows the OH yields referenced with respect to ethene (calculated using Eq. 3):

$$\text{Relative OH yield} = A \text{ factor}_{(reagent)} : A \text{ factor}_{(ethene)} \tag{3}$$

4 Discussion

4.1 Time-resolved model-measurement comparison

Under conditions optimised for complete conversion of RO_2 radicals to OH in a FAGE cell with added NO, i.e. very long reaction times, the yield of HO_2 from a number of alkene-derived RO_2 species compares favourably to the MCMv3.2 predictions of the OH yield determined using Eq. (4) after a reaction time of 9.8 ms as shown in Fig. 4 and Table 2, suggesting that the yield of HO_2 from other RO_2 species not measured here can be derived with some confidence from MCM predictions.

$$\text{MCM OH yield} = \frac{\text{modelled [OH] generated}}{\text{model initialised [RO}_2\text{]}} \tag{4}$$

For $> C_3$ alkane-derived RO_2 species, the MCM also predicts a non-zero HO_2 yield. For these species, reaction with NO produces an alkoxy radical which can react with O_2 or isomerise forming a β-hydroxyalkylperoxy radical in the presence of O_2, which for the case of n-butane derived peroxy radical is:

$$C_4H_9O_2 + NO \rightarrow C_4H_9O + NO_2 \tag{R20}$$

$$C_4H_9O \xrightarrow{\text{isom.}} (HO)C_4H_8 \tag{R21}$$

$$(HO)C_4H_8 + O_2 \rightarrow (HO)C_4H_8O_2 \tag{R22}$$
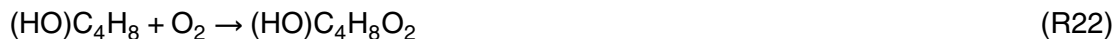
The alkoxy radical, C_4H_9O, may also react with NO under FAGE conditions:

$$C_4H_9O + NO \rightarrow C_4H_9ONO \tag{R23}$$

As shown in Reactions (R8)–(R11) the β-hydroxyalkylperoxy radical can react further with NO and decompose rapidly in the presence of O_2 to form HO_2. However, as seen in Fig. 4, the MCM over-predicts the yield of HO_2 at 298 K from n-pentane and cyclo-hexane derived peroxy radicals, and under-predicts the OH yield from n-butane-derived

6267

alkanes. The modelled to measured agreement for *n*-pentane and cyclohexane derived RO_2 radicals can be improved if the rate coefficient for isomerisation (Reaction R21) is reduced by assuming a lower temperature; it was found by varying the temperature in the model that 255 K provided the best agreement for all RO_2 species considered (Fig. 4). In the case of cyclohexane, the rate coefficient for isomerisation (taken from the MCMv3.2) decreases from $6.3 \times 10^4 \, s^{-1}$ to $2.1 \times 10^3 \, s^{-1}$ as the temperature was reduced from 298 K to 255 K. Stevens et al. (1994) report a temperature of 245 K within the Penn. State FAGE instrument as an airstream enters the detection cell and accelerates to velocities of $> 300 \, ms^{-1}$; at the laser detection axis the velocity is reduced to $\sim 50 \, ms^{-1}$ and the air temperature increases to ambient levels once more. Similarly, measurements of rotational temperatures and computational fluid dynamic (CFD) calculations performed to determine the temperature and density profiles of an airstream within the Leeds FAGE detection cells (Fig. 1a) suggest that air temperatures drop as low as 25 K in the first 2 cm in the detection cell beneath the pinhole as the airstream expands supersonically and reaches velocities of $750 \, ms^{-1}$ before slowing and increasing back to ambient temperatures at the detection axis (Creasey et al., 1997b). Taking these temperature profiles into account, it is expected that the mean temperature experienced between pinhole and the detection axis will be below ambient and if this is the case the rate coefficient for isomerisation will slow considerably (Orlando et al., 2003). At lower temperatures the reaction between an alkoxy radical and NO (Reaction R19) can begin to compete with the isomerisation (Reaction R21) and can, as a result, lower the overall OH yield observed from these RO_2 radicals. This effect reduces the agreement between the experimental and modelled OH yield from *n*-butane-derived RO_2 further suggesting that the rate coefficient for isomerisation of the C_4H_9O alkoxy radical may actually be faster than assumed in the model. There is very little information on the temperature dependence associated with the rate of β hydroxyalkoxy decomposition in the literature. A theoretical temperature dependence for the rate of decomposition of

Title Page

Abstract | Introduction

Conclusions | References

Tables | Figures

◄ | ►

◄ | ►

Back | Close

Full Screen / Esc

ethene-derived β-hydroxyalkoxy radical has been reported (Kukui and Le Bras, 2001):

$$k_{\text{decomp.}} = 1.1 \times 10^{13}\,[\text{s}^{-1}] \cdot e^{\frac{-41.84[\text{KJ mole}^{-1}]}{RT}} \tag{5}$$

When this temperature dependence is included in model calculations, assuming a temperature of 255 K, the OH yield predicted is reduced by $\sim 10\%$ from calculations assuming a temperature of 298 K (Fig. 4) as the rate coefficient for decomposition decreases from $5.1 \times 10^5\,\text{s}^{-1}$ to $3.0 \times 10^4\,\text{s}^{-1}$. Although likely to be similar to that of the ethene-dervied alkoxy radical, no information on the temperature dependence of isoprene-derived alkoxy radical decomposition exists in the literature so the impact on the OH yield at reduced temperatures is not considered here.

Magnitude of the interference for fieldwork instruments

For the three fieldwork FAGE cells tested (Fig. 1) which have different residence times and, hence reaction times for RO_2 conversion to OH, the yield of OH from the alkene-derived RO_2 radicals was variable. The best agreement between the MCM predictions and experimental results occurs if a contact time (and [NO]) of ~ 0.9 ms (and 1×10^{14} molecule cm^{-3}), ~ 1.9 ms (and 1×10^{14} molecule cm^{-3}) and ~ 60 ms (and 1×10^{13} molecule cm^{-3}) is assumed for cell A, cell B and cell C (Fig. 1) respectively; at a temperature of 255 K. For cell A, a residence time from pinhole to detection region of < 1 ms has been calculated using CFD (Creasey et al., 1997b) and compares favourably to the estimated contact time of 0.9 ms (estimated from the agreement between the experimental relative yields and those modelled at 0.9 ms, Fig. 5, upper panel). As it is difficult to calculate the cell residence absolutely, due to the free-jet expansion that occurs, comparison of the yields with model predictions provides a means to gauge the time spent between the NO injection region and detection region experimentally. Uncertainty in the residence time may arise, however, if the NO injected into the cell does not fully mix with the sampled air stream or if the mean temperature of the airstream is not considered and ambient temperature is assumed. Qualitatively, the

extent of the interference suffered is directly proportional to residence time within the jet and inversely proportional to the mean temperature experienced by the jet (Eq. 6). The level of interference suffered with respect to [NO] is complex. Increasing the concentration will increase the rates of Reactions (R3) and (R5) but also increases the

5 rate of Reaction (R19). For alkoxy radicals which display a strong temperature dependence with respect to isomerisation, as is the case for the alkoxy radical derived from cyclohexane (CHEXO), increasing NO concentrations beyond a certain concentration may actually lead to a reduction in the level of interference observed as R19 begins to competes effectively with R21. Model simulations looking at the yield of OH from

10 cyclohexane-derived RO_2 radicals predict that at a residence time of 9.8 ms (time over which time-resolved experiments were run) the yield of OH will increase with increasing [NO] until a NO concentration of 1.2×10^{14} molecule cm^{-3} is reached and then the yield will begin to decrease as [NO] increases further. Note, if the residence time is increased, less NO is required to achieve the maximum yield and vice versa. Under the

15 experimental conditions discussed in this paper (i.e. [NO] $\leq 1 \times 10^{14}$ molecule cm^{-3}), the OH yield should have been directly proportional to [NO]:

$$\text{Interference } \alpha \frac{\text{Residence time} \cdot [\text{NO}]}{\text{Temperature}} \qquad (6)$$

Fuchs et al. (2011) observed a large under-prediction of the OH yield from cyclohexane-derived RO_2 radicals in the presence of NO and suggested that the model

20 under-prediction for the yield of OH from this species may reflect a missing ring opening mechanism in the MCM which could promote further HO_2 formation. Fuchs et al. (2011) used MCMv3.1 which did not contain a ring opening mechanism to estimate the expected level of interference in the Julich FAGE system. An additional degradation pathway for CHEXO which includes a ring opening route, is included in

25 MCMv3.2 leading to the yield of HO_2 (and ultimately OH, following further reaction) from cyclohexane-derived RO_2 radicals approximately doubling when switching from MCMv3.1 to MCMv3.2 chemistry.

A lower effective yield of OH from cyclohexane derived RO_2 radicals (relative to ethene derived RO_2 radicals) was observed in the time-resolved experiments (Table 2) compared to experiments on cell C (Table 1). The model is able to reproduce the relative yields observed in both experiments if the concentration of NO that mixes into the jet expansion in cell C is lower (by a factor of 10) than the [NO] that was actually injected; the required reduction in modelled NO for cell C was consistent for all RO_2 species studied. Under this scenario, the competition of R19 with R21 is reduced leading to an increased yield of OH in cell C experiments.

4.2 Minimising the RO_2 interference further

As highlighted in Table 1, a decrease in the amount of NO injected into the cell reduces the OH yield from ethene-derived RO_2 radicals. Reducing the sensitivity of the instrument to the interference, however, leads to a concomitant reduction in HO_2 sensitivity. As only one NO molecule is required to titrate one HO_2 radical to OH, whilst two or more are required for RO_2 to OH titration, it is possible to begin to discriminate between HO_2 and RO_2 by reducing the amount of NO mixed into the jet as shown in Fig. 6. At an NO concentration of 1×10^{13} molecule cm^{-3}, approximately twenty HO_2 radicals titrate to OH for one RO_2i radical conversion to OH; determined from the ratio: relative OH yield (propane): relative OH yield (ethene) with "relative OH yield" calculated using Eq. (1). At this NO concentration the 5 min limit of detection of the instrument for HO_2 will be $\sim 4 \times 10^6$ molecule cm^{-3} and, although higher than detection limits from earlier campaigns (e.g. the HO_2 LOD during the SOAPEX campaign which took place in Cape Grim in Australia was 5.4×10^5 molecule cm^{-3} for 2.5 min integration time) (Creasey et al., 2003), the instrument remains sufficiently sensitive for ambient HO_2 detection with minimal RO_2 interference ($\sim 5\%$). It should be noted that good agreement between the MCMv3.2 model and observations can only be achieved if it is assumed that 5.5 times less NO is mixed fully into the air sample within the FAGE cell than is actually injected.

As demonstrated by Fig. 6, by varying the amount of NO injected it is possible to switch from conditions where certain RO_2 types are efficiently converted to OH (NO $> 5 \times 10^{13}$ molecule cm^{-3}) to conditions were the conversion is poor (NO $< 1 \times 10^{13}$ molecule cm^{-3}). With knowledge of the conversion efficiency of RO_2 and HO_2 at different NO concentrations, changing the NO flow during ambient measurements can selectively provide a measurement of the concentration of RO_2i and HO_2 by solving simultaneous Eqs. (7 and 8):

$$HO_x \text{ signal}_{\text{low [NO]}} = C_{HO_2, \text{ low [NO]}} \cdot ([HO_2] + \alpha_{\text{low [NO]}}[RO_2i]) \tag{7}$$

$$HO_x \text{ signal}_{\text{high [NO]}} = C_{HO_2, \text{ high [NO]}} \cdot ([HO_2] + \alpha_{\text{high [NO]}}[RO_2i]) \tag{8}$$

Where HO_x signal is the fluorescence signal observed in cts s^{-1} mW^{-1}, C_{HO_2} is the sensitivity of the instrument to HO_2 (determined by calibration) at a particular NO flow in units of cm^3 molecule^{-1} ct s^{-1} mW^{-1} and α is the mean fractional contribution of RO_2i at a selected [NO].

During a recent field project, the Clean air for London campaign (ClearfLo), this approach was adopted during ambient measurements. The NO concentration injected into a FAGE cell (cell type A) used during the campaign for sequential measurements of OH and HO_2 was varied between ~ 1 and 9×10^{13} molecule cm^{-3}; a measurement of the total [RO_2] was determined simultaneously using the RO_xLIF cell C operating in RO_x mode. The campaign average diurnal profile of HO_2, alkene/aromatic or long-chain alkane-derived RO_2 and short-chain alkane-derived RO_2 radicals selectively measured is provided in Fig. 7. An alternative approach to partial speciation of RO_2 radical classes would be to use two FAGE cells in which the RO_2 interference is minimised in the first (e.g. cell A, run at a low [NO]) and maximised in the second (e.g. cell C, HO_x mode, run at a high [NO]).

4.3 Impact on previous field studies

The University of Leeds ground-based FAGE instrument has been operational since 1996 and has taken part in 17 campaigns. In some of the earlier campaigns good conversion of HO_2 to OH was achieved as two independent cells were used (Creasey et al., 2002; Creasey et al., 2003; Smith et al., 2006), with the conditions of one cell optimised for HO_2 detection, and so a significant portion of interfering RO_2i, if present, may also have been titrated to OH, constituting an interference. Many of the previous campaigns took place under relatively clean, unpolluted conditions, for example EASE-96 (Carslaw et al., 1999a), EASE-97 (Creasey et al., 2002), SOAPEX (Creasey et al., 2003), NAMBLEX (Smith et al., 2006), CHABLIS (Bloss et al., 2010), RHAMBLE (Whalley et al., 2010) where the concentrations of RO_2i are likely low and methyl peroxy radicals, which do not give an interference (Ren et al., 2004), were expected to be the dominant RO_2 species; e.g. during EASE-96 the model predicted that 92 % of peroxy radicals present were either HO_2 (53 %) or CH_3O_2 (39 %) during unpolluted conditions (Carslaw et al., 1999a). Similarly, for the SOS project (Vaughan et al., 2012), which took place in Cape Verde, models predicted that $\sim$ 90 % of peroxy radicals were either HO_2 or CH_3O_2. In general, models run for these campaigns tended to over-predict HO_2 despite additional HO_2 loss mechanisms such as reaction with halogen oxides and/or heterogeneous loss to aerosol surfaces in the model description. In contrast, under polluted, urban conditions (e.g. PUMA, Heard et al., 2004, TORCH-1, Emmerson et al., 2007) models either significantly under-predicted HO_2 observations (PUMA) (Emmerson et al., 2005) or were in relatively good agreement (TORCH-1)(Emmerson et al., 2007). If elevated concentrations of alkene-derived, aromatic-derived and higher-alkane derived RO_2 species were present, the true ambient HO_2 concentrations, as opposed to HO_2^*, were likely lower than reported. It is possible, although difficult to verify without observations of speciated RO_2 that the conclusions drawn from these observations, for example, that additional HO_2 sources in models are required to replicate observations, may be in error.

Sensitivity of Laser Induced Fluorescence instruments

L. K. Whalley et al.

Title Page

Abstract	Introduction
Conclusions	References
Tables	Figures

◀ | ▶|

◀ | ▶

Back | Close

Full Screen / Esc

Printer-friendly Version

Interactive Discussion

Under the operating conditions employed during the OP3 campaign, the instrument was relatively insensitive to detection of RO_2 species. The experiments presented here reveal a 17 % yield of OH due to the decomposition of ethene-derived RO_2 in the presence of NO in the FAGE detection cell under OP3 conditions. This provides an upper limit to the HO_2 yield from RO_2 species during OP3 as, under conditions in which the interference signal was maximised (Sect. 3.2), ethene-derived RO_2 species provided the largest HO_2 yield compared with other RO_2 species. Model simulations (Whalley et al., 2011) suggested that up to 2.1×10^8 molecule cm^{-3} of potentially interfering RO_2 species were present at solar noon during OP3 (with isoprene derived peroxy radicals contributing ~ 60 % to this total), and thus up to 3.5×10^7 molecule cm^{-3} of the HO_2 concentration may be attributed to these species (~ 10 % of the total HO_2 signal observed (Whalley et al., 2011)). Model comparisons with the radical measurements made during the campaign demonstrated a large missing OH source and over-predicted the HO_2 observations. The small positive bias on the HO_2 observations, owing to the small yield of HO_2 from RO_2 species, only serves to reduce the modelled to measured agreement further. For the HCCT-2010 campaign, the potential impact of the interfering RO_2 species is greater (Table 1, Fig. 5) owing to the smaller cell (with a longer inlet) and longer residence time employed. The campaign took place in a pine forest, close to the summit of Mount Schmücke in the Thüringer Wald mountain range in East Germany, during September and October 2010. VOC measurements were made downwind of the measurement site. Only low concentrations of isoprene (50 pptv) were detected, however, suggesting that the concentration of RO_2i were also low.

5   Conclusions and further work

Recent studies conducted on a number of different fluorescence cells used in the FAGE instrument at Leeds have demonstrated that alkene- and aromatic-derived RO_2 species can yield appreciable quantities of OH upon addition of NO in FAGE detection cells and, therefore, positively bias HO_2 observations if left uncorrected. Many FAGE groups

now report HO_2^* for comparison with atmospheric chemistry box models to include any interference from RO_2i. As demonstrated in this study, the magnitude of this interference is critically dependent on the cell design, quantity of NO used in the titration, the residence time and mean temperature of the air stream within the FAGE cell. The interference may be minimised by reducing NO concentrations and/or residence time, and although such a reduction will also reduce the sensitivity of the instrument to HO_2 (albeit to a lesser extent than the reduction in the sensitivity to RO_2 radicals) it will still be possible to detect ambient levels HO_2 using FAGE.

In laboratory, laser-flash photolysis experiments, under conditions optimised for complete conversion of RO_2 radicals to OH in a FAGE cell, the yield of HO_2 from a number of alkene-derived RO_2 species could be measured, and compared favourably with MCMv3.2 predictions. This suggests that the yield of HO_2 from other alkene-derived or aromatic-derived RO_2 species not tested here, but which are expected to exhibit high yields, could be determined from MCM predictions. The ability to discriminate between HO_2 and RO_2i radicals, as illustrated for the ClearfLo project, is not only of great value for field measurements (and subsequent model comparisons), but such instrumentation may be used to selectively determine the yield of HO_2 in laboratory experiments under conditions where RO_2 radicals may also be present. Important applications, for example, would be the experimental verification of a significant prompt HO_2 yield from OH initialised isoprene oxidation, as proposed by Peeters et al. (2009) or prompt HO_2 yields from OH initialised oxidation of aromatics (Nehr et al., 2012).

This study demonstrates that some of the previous HO_2 measurements that depend upon chemical titration to OH by NO may suffer an interference due to partial detection of RO_2 radicals. Under conditions where there are significant alkene, aromatic or long-chain alkanes present, the HO_2^* concentration which was measured will have been higher than the HO_2 concentration that was actually present. Models have over-estimated HO_2 concentrations under such conditions, and this over-estimation would only increase if the observations of HO_2 were corrected for the interference suggesting there is a major gap in our understanding of the chemistry controlling these radicals.

Title Page

Abstract | Introduction

Conclusions | References

Tables | Figures

◄ | ►

◄ | ►

Back | Close

Full Screen / Esc

Printer-friendly Version

Interactive Discussion

Supplementary material related to this article is available online at: http://www.atmos-meas-tech-discuss.net/6/6249/2013/ amtd-6-6249-2013-supplement.pdf.

References

Atkinson, R., Baulch, D. L., Cox, R. A., Hampson, R. F., Kerr, J. A., Rossi, M. J., and Troe, J.: Evaluated kinetic, photochemical and heterogeneous data for atmospheric chemistry, 5. IU-PAC subcommittee on gas kinetic data evaluation for atmospheric chemistry, J. Phys. Chem. Ref. Data, 26, 521–1011, 1997.

Atkinson, R., Baulch, D. L., Cox, R. A., Crowley, J. N., Hampson, R. F., Hynes, R. G., Jenkin, M. E., Rossi, M. J., and Troe, J.: Evaluated kinetic and photochemical data for atmospheric chemistry: Volume I – gas phase reactions of O_x, HO_x, NO_x and SO_x species, Atmos. Chem. Phys., 4, 1461–1738, doi:10.5194/acp-4-1461-2004, 2004.

Bloss, C., Wagner, V., Jenkin, M. E., Volkamer, R., Bloss, W. J., Lee, J. D., Heard, D. E., Wirtz, K., Martin-Reviejo, M., Rea, G., Wenger, J. C., and Pilling, M. J.: Development of a detailed chemical mechanism (MCMv3.1) for the atmospheric oxidation of aromatic hydrocarbons, Atmos. Chem. Phys., 5, 641–664, doi:10.5194/acp-5-641-2005, 2005.

Bloss, W. J., Camredon, M., Lee, J. D., Heard, D. E., Plane, J. M. C., Saiz-Lopez, A., Bauguitte, S. J.-B., Salmon, R. A., and Jones, A. E.: Coupling of HO_x, NO_x and halogen chemistry in the antarctic boundary layer, Atmos. Chem. Phys., 10, 10187–10209, doi:10.5194/acp-10-10187-2010, 2010.

Carslaw, N., Creasey, D. J., Heard, D. E., Lewis, A. C., McQuaid, J. B., Pilling, M. J., Monks, P. S., Bandy, B. J., and Penkett, S. A.: Modeling OH, HO_2, and RO_2 radicals in the marine boundary layer – 1. Model construction and comparison with field measurements, J. Geophys. Res.-Atmos., 104, 30241–30255, doi:10.1029/1999jd900783, 1999a.

Sensitivity of Laser Induced Fluorescence instruments

L. K. Whalley et al.

Title Page

Abstract	Introduction
Conclusions	References
Tables	Figures

|◄ | ►|

◄ | ►

Back | Close

Full Screen / Esc

Printer-friendly Version

Interactive Discussion

Carslaw, N., Jacobs, P. J., and Pilling, M. J.: Modeling OH, HO$_2$, and RO$_2$ radicals in the marine boundary layer 2. Mechanism reduction and uncertainty analysis, J. Geophys. Res.-Atmos., 104, 30257–30273, doi:10.1029/1999jd900782, 1999b.

Cleary, P. A., Romero, M. T. B., Blitz, M. A., Heard, D. E., Pilling, M. J., Seakins, P. W., and Wang, L.: Determination of the temperature and pressure dependence of the reaction OH + C$_2$H$_4$ from 200–400 K using experimental and master equation analyses, Phys. Chem. Chem. Phys., 8, 5633–5642, doi:10.1039/B612127f, 2006.

Commane, R., Floquet, C. F. A., Ingham, T., Stone, D., Evans, M. J., and Heard, D. E.: Observations of OH and HO$_2$ radicals over West Africa, Atmos. Chem. Phys., 10, 8783–8801, doi:10.5194/acp-10-8783-2010, 2010.

Creasey, D. J., HalfordMaw, P. A., Heard, D. E., Pilling, M. J., and Whitaker, B. J.: Implementation and initial deployment of a field instrument for measurement of OH and HO$_2$ in the troposphere by laser-induced fluorescence, J. Chem. Soc. Faraday T., 93, 2907–2913, doi:10.1039/A701469d, 1997a.

Creasey, D. J., Heard, D. E., Pilling, M. J., Whitaker, B. J., Berzins, M., and Fairlie, R.: Visualisation of a supersonic free-jet expansion using laser-induced fluorescence spectroscopy: Application to the measurement of rate constants at ultralow temperatures, Appl. Phys. B-Lasers O., 65, 375–391, doi:10.1007/s003400050285, 1997b.

Creasey, D. J., Heard, D. E., and Lee, J. D.: OH and HO$_2$ measurements in a forested region of north-western Greece, Atmos. Environ., 35, 4713–4724, doi:10.1016/S1352-2310(01)00090-5, 2001.

Creasey, D. J., Heard, D. E., and Lee, J. D.: Eastern Atlantic Spring Experiment 1997 (EASE97) 1. Measurements of OH and HO$_2$ concentrations at Mace Head, Ireland, J. Geophys. Res.-Atmos., 107, 4091, doi:10.1029/2001jd000892, 2002.

Creasey, D. J., Evans, G. E., Heard, D. E., and Lee, J. D.: Measurements of OH and HO$_2$ concentrations in the Southern Ocean marine boundary layer, J. Geophys. Res.-Atmos., 108, 4475, doi:10.1029/2002jd003206, 2003.

Davis, D. D., Rodgers, M. O., Fischer, S. D., and Asai, K.: An experimental assessment of the O$_3$/H$_2$O interference problem in the detection of natural levels of OH via laser induced fluorescence, Geophys. Res. Lett., 8, 69–72, 1981.

Emmerson, K. M., Carslaw, N., Carpenter, L. J., E., H. D., Lee, J. D., and Pilling, M. J.: Urban atmospheric chemistry during the PUMA Campaign 1: Comparison of modelled OH and HO$_2$ concentrations with measurements, J. Atmos. Chem., 52, 143–164, 2005.

Sensitivity of Laser Induced Fluorescence instruments

L. K. Whalley et al.

Title Page

Abstract	Introduction
Conclusions	References
Tables	Figures

|◄ ►|

◄ ►

Back Close

Full Screen / Esc

Printer-friendly Version

Interactive Discussion

Emmerson, K. M., Carslaw, N., Carslaw, D. C., Lee, J. D., McFiggans, G., Bloss, W. J., Grave-stock, T., Heard, D. E., Hopkins, J., Ingham, T., Pilling, M. J., Smith, S. C., Jacob, M., and Monks, P. S.: Free radical modelling studies during the UK TORCH Campaign in Summer 2003, Atmos. Chem. Phys., 7, 167–181, doi:10.5194/acp-7-167-2007, 2007.

Faloona, I., Tan, D., Brune, W., Hurst, J., Barket, D., Couch, T. L., Shepson, P., Apel, E., Riemer, D., Thornberry, T., Carroll, M. A., Sillman, S., Keeler, G. J., Sagady, J., Hooper, D., and Paterson, K.: Nighttime observations of anomalously high levels of hydroxyl radicals above a deciduous forest canopy, J. Geophys. Res.-Atmos., 106, 24315–24333, doi:10.1029/2000jd900691, 2001.

Fuchs, H., Holland, F., and Hofzumahaus, A.: Measurement of tropospheric RO_2 and HO_2 radicals by a laser-induced fluorescence instrument, Rev. Sci. Instrum., 79, 084104, doi:10.1063/1.29687121, 2008.

Fuchs, H., Bohn, B., Hofzumahaus, A., Holland, F., Lu, K. D., Nehr, S., Rohrer, F., and Wah-ner, A.: Detection of HO_2 by laser-induced fluorescence: calibration and interferences from RO_2 radicals, Atmos. Meas. Tech., 4, 1209–1225, doi:10.5194/amt-4-1209-2011, 2011.

Fuchs, H., Dorn, H.-P., Bachner, M., Bohn, B., Brauers, T., Gomm, S., Hofzumahaus, A., Hol-land, F., Nehr, S., Rohrer, F., Tillmann, R., and Wahner, A.: Comparison of OH concentration measurements by DOAS and LIF during SAPHIR chamber experiments at high OH reactiv-ity and low NO concentration, Atmos. Meas. Tech., 5, 1611–1626, doi:10.5194/amt-5-1611-2012, 2012.

Hanisco, T. F., Smith, J. B., Stimpfle, R. M., Wilmouth, D. M., Anderson, J. G., Richard, E. C., and Bui, T. P.: In situ observations of HO_2 and OH obtained on the NASA ER-2 in the high-ClO conditions of the 1999/2000 Arctic polar vortex, J. Geophys. Res.-Atmos., 107, 8283, doi:10.1029/2001jd001024, 2002.

Hard, T. M., Obrien, R. J., Cook, T. B., and Tsongas, G. A.: Interference Suppression in OH Fluorescence Detection, Appl. Optics, 18, 3216–3217, doi:10.1364/Ao.18.003216, 1979.

Hard, T. M., Obrien, R. J., Chan, C. Y., and Mehrabzadeh, A. A.: Tropospheric Free-Radical De-termination by Fage, Environ. Sci. Technol., 18, 768–777, doi:10.1021/Es00128a009, 1984.

Heard, D. E. and Pilling, M. J.: Measurement of OH and HO_2 in the troposphere, Chem. Rev., 103, 5163–5198, doi:10.1021/Cr020522s, 2003.

Heard, D. E., Carpenter, L. J., Creasey, D. J., Hopkins, J. R., Lee, J. D., Lewis, A. C., Pilling, M. J., Seakins, P. W., Carslaw, N., and Emmerson, K. M.: High levels of the

hydroxyl radical in the winter urban troposphere, Geophys. Res. Lett., 31, L18112, doi:10.1029/2004gl020544, 2004.

Heicklen, J.: The Decomposition of Alkyl Nitrites and the Reactions of Alkoxyl Radicals, in: Advances in Photochemistry, edited by: Volman, D. H., Hammond, G. S., and Gollnick, K., Vol. 14, John Wiley & Sons, Inc., Hoboken, NJ, USA, doi:10.1002/9780470133446.ch4, 2007.

Hewitt, C. N., Lee, J. D., MacKenzie, A. R., Barkley, M. P., Carslaw, N., Carver, G. D., Chappell, N. A., Coe, H., Collier, C., Commane, R., Davies, F., Davison, B., DiCarlo, P., Di Marco, C. F., Dorsey, J. R., Edwards, P. M., Evans, M. J., Fowler, D., Furneaux, K. L., Gallagher, M., Guenther, A., Heard, D. E., Helfter, C., Hopkins, J., Ingham, T., Irwin, M., Jones, C., Karunaharan, A., Langford, B., Lewis, A. C., Lim, S. F., MacDonald, S. M., Mahajan, A. S., Malpass, S., McFiggans, G., Mills, G., Misztal, P., Moller, S., Monks, P. S., Nemitz, E., Nicolas-Perea, V., Oetjen, H., Oram, D. E., Palmer, P. I., Phillips, G. J., Pike, R., Plane, J. M. C., Pugh, T., Pyle, J. A., Reeves, C. E., Robinson, N. H., Stewart, D., Stone, D., Whalley, L. K., and Yin, X.: Overview: oxidant and particle photochemical processes above a south-east Asian tropical rainforest (the OP3 project): introduction, rationale, location characteristics and tools, Atmos. Chem. Phys., 10, 169–199, doi:10.5194/acp-10-169-2010, 2010.

Hofzumahaus, A., Aschmutat, U., Hessling, M., Holland, F., and Ehhalt, D. H.: The measurement of tropospheric OH radicals by laser-induced fluorescence spectroscopy during the POPCORN field campaign, Geophys. Res. Lett., 23, 2541–2544, doi:10.1029/96gl02205, 1996.

Holland, F., Hofzumahaus, A., Schafer, R., Kraus, A., and Patz, H. W.: Measurements of OH and HO_2 radical concentrations and photolysis frequencies during BERLIOZ, J. Geophys. Res.-Atmos., 108, 8246, doi:10.1029/2001jd001393, 2003.

Ianni, J. C.: available at: www.kintecus.com (last access: 10 June 2013), in Windows version 2.80 ed., 2002.

Jenkin, M. E., Saunders, S. M., and Pilling, M. J.: The tropospheric degradation of volatile organic compounds: a protocol for mechanism development, Atmos. Environ., 31, 81–104, doi:10.1016/S1352-2310(96)00105-7, 1997.

Jenkin, M. E., Saunders, S. M., Wagner, V., and Pilling, M. J.: Protocol for the development of the Master Chemical Mechanism, MCM v3 (Part B): tropospheric degradation of aromatic volatile organic compounds, Atmos. Chem. Phys., 3, 181–193, doi:10.5194/acp-3-181-2003, 2003.

Title Page

Abstract | Introduction

Conclusions | References

Tables | Figures

|◄ | ►|

◄ | ►

Back | Close

Full Screen / Esc

Printer-friendly Version

Interactive Discussion

Kanaya, Y., Sadanaga, Y., Matsumoto, J., Sharma, U. K., Hirokawa, J., Kajii, Y., and Akimoto, H.: Nighttime observation of the HO_2 radical by an LIF instrument at Oki island, Japan, and its possible origins, Geophys. Res. Lett., 26, 2179–2182, doi:10.1029/1999gl900475, 1999.

Kukui, A. and Le Bras, G.: Theoretical study of the thermal decomposition of several beta-chloroalkoxy radicals, Phys. Chem. Chem. Phys., 3, 175–178, doi:10.1039/B007644i, 2001.

Lu, K. D., Rohrer, F., Holland, F., Fuchs, H., Bohn, B., Brauers, T., Chang, C. C., Häseler, R., Hu, M., Kita, K., Kondo, Y., Li, X., Lou, S. R., Nehr, S., Shao, M., Zeng, L. M., Wahner, A., Zhang, Y. H., and Hofzumahaus, A.: Observation and modelling of OH and HO_2 concentrations in the Pearl River Delta 2006: a missing OH source in a VOC rich atmosphere, Atmos. Chem. Phys., 12, 1541–1569, doi:10.5194/acp-12-1541-2012, 2012.

Mao, J., Ren, X., Zhang, L., Van Duin, D. M., Cohen, R. C., Park, J.-H., Goldstein, A. H., Paulot, F., Beaver, M. R., Crounse, J. D., Wennberg, P. O., DiGangi, J. P., Henry, S. B., Keutsch, F. N., Park, C., Schade, G. W., Wolfe, G. M., Thornton, J. A., and Brune, W. H.: Insights into hydroxyl measurements and atmospheric oxidation in a California forest, Atmos. Chem. Phys., 12, 8009–8020, doi:10.5194/acp-12-8009-2012, 2012.

Mather, J. H., Stevens, P. S., and Brune, W. H.: OH and HO_2 measurements using laser-induced fluorescence, J. Geophys. Res.-Atmos., 102, 6427–6436, doi:10.1029/96jd01702, 1997.

Nehr, S., Bohn, B., and Wahner, A.: Prompt HO_2 formation following the reaction of OH with aromatic compounds under atmospheric conditions, J. Phys. Chem. A, 116, 6015–6026, doi:10.1021/Jp210946y, 2012.

Orlando, J. J., Tyndall, G. S., and Wallington, T. J.: The atmospheric chemistry of alkoxy radicals, Chem. Rev., 103, 4657–4689, doi:10.1021/Cr020527p, 2003.

Ortgies, G., Gericke, K. H., and Comes, F. J.: Is UV laser-induced fluorescence a method to monitor tropospheric OH?, Geophys. Res. Lett., 7, 905–908, doi:10.1029/Gl007i011p00905, 1980.

Peeters, J., Nguyen, T. L., and Vereecken, L.: HO_x radical regeneration in the oxidation of isoprene, Phys. Chem. Chem. Phys., 11, 5935–5939, 2009.

Ren, X. R., Harder, H., Martinez, M., Faloona, I. C., Tan, D., Lesher, R. L., Di Carlo, P., Simpas, J. B., and Brune, W. H.: Interference testing for atmospheric HO_x measurements by laser-induced fluorescence, J. Atmos. Chem., 47, 169–190, doi:10.1023/B:Joch.0000021037.46866.81, 2004.

Title Page

Abstract | Introduction

Conclusions | References

Tables | Figures

◄ | ►►

◄ | ►

Back | Close

Full Screen / Esc

Printer-friendly Version

Interactive Discussion

Sadanaga, Y., Yoshino, A., Watanabe, K., Yoshioka, A., Wakazono, Y., Kanaya, Y., and Kajii, Y.: Development of a measurement system of OH reactivity in the atmosphere using a laser-induced pupm and probe technique, Rev. Sci. Instr., 75, 2648–2655, 2004.

Saunders, S. M., Jenkin, M. E., Derwent, R. G., and Pilling, M. J.: Protocol for the development of the Master Chemical Mechanism, MCM v3 (Part A): tropospheric degradation of non-aromatic volatile organic compounds, Atmos. Chem. Phys., 3, 161–180, doi:10.5194/acp-3-161-2003, 2003.

Shirinzadeh, B., Wang, C. C., and Deng, D. Q.: Pressure-Dependence of Ozone Interference in the Laser Fluorescence Measurements of OH in the Atmosphere, Appl. Optics, 26, 2102–2105, 1987.

Smith, S. C., Lee, J. D., Bloss, W. J., Johnson, G. P., Ingham, T., and Heard, D. E.: Concentrations of OH and HO_2 radicals during NAMBLEX: measurements and steady state analysis, Atmos. Chem. Phys., 6, 1435–1453, doi:10.5194/acp-6-1435-2006, 2006.

Stevens, P. S., Mather, J. H., and Brune, W. H.: Measurement of tropospheric OH and HO_2 by laser-induced fluorescence at low-pressure, J. Geophys. Res.-Atmos., 99, 3543–3557, doi:10.1029/93jd03342, 1994.

Stone, D., Whalley, L. K., and Heard, D. E.: Tropospheric OH and HO_2 radicals: field measurements and model comparisons, Chem. Soc. Rev., 41, 6348–6404, doi:10.1039/C2cs35140d, 2012.

Vaughan, S., Ingham, T., Whalley, L. K., Stone, D., Evans, M. J., Read, K. A., Lee, J. D., Moller, S. J., Carpenter, L. J., Lewis, A. C., Fleming, Z. L., and Heard, D. E.: Seasonal observations of OH and HO_2 in the remote tropical marine boundary layer, Atmos. Chem. Phys., 12, 2149–2172, doi:10.5194/acp-12-2149-2012, 2012.

Whalley, L. K., Furneaux, K. L., Goddard, A., Lee, J. D., Mahajan, A., Oetjen, H., Read, K. A., Kaaden, N., Carpenter, L. J., Lewis, A. C., Plane, J. M. C., Saltzman, E. S., Wiedensohler, A., and Heard, D. E.: The chemistry of OH and HO_2 radicals in the boundary layer over the tropical Atlantic Ocean, Atmos. Chem. Phys., 10, 1555–1576, doi:10.5194/acp-10-1555-2010, 2010.

Whalley, L. K., Edwards, P. M., Furneaux, K. L., Goddard, A., Ingham, T., Evans, M. J., Stone, D., Hopkins, J. R., Jones, C. E., Karunaharan, A., Lee, J. D., Lewis, A. C., Monks, P. S., Moller, S. J., and Heard, D. E.: Quantifying the magnitude of a missing hydroxyl radical source in a tropical rainforest, Atmos. Chem. Phys., 11, 7223–7233, doi:10.5194/acp-11-7223-2011, 2011.

Whalley, L. K., Stone, D., George, I., Mertes, S., Van Pinxteren, D., Fomba, K. W., Herrmann, H., and Heard, D. E.: The influence of clouds on radical concentrations: observations of OH and HO_2 during the Hill Cap Cloud Thuringer (HCCT) campaign in 2010, to be submitted, 2013.

Sensitivity of Laser Induced Fluorescence instruments

L. K. Whalley et al.

Title Page

Abstract	Introduction
Conclusions	References
Tables	Figures

Back | Close

Full Screen / Esc

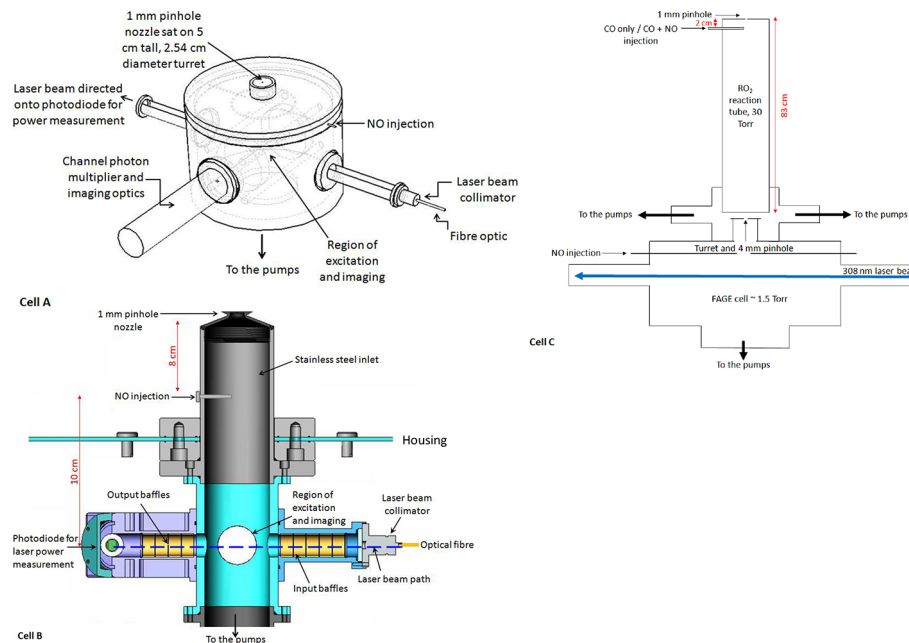Printer-friendly Version

Interactive Discussion

Table 1. Experimentally determined OH yields (derived using Eq. 1) from peroxy radicals ($RO_2 \rightarrow HO_2 \rightarrow OH$) in continuous flow experiments for FAGE cells operated under fieldwork conditions.

Source of peroxy radicals	Flow of NO (SCCM)	Cell A, OH yield Residence time: $\sim 0.9\,\mathrm{ms}$[1] Typical NO flow used during fieldwork: 50 SCCM[2] Flow rate through pinhole: 4.8 SLM Cell Pressure: 0.9 Torr	Cell B, OH yield Residence time: $\sim 1.9\,\mathrm{ms}$[3] Typical NO flow used during fieldwork: 10 SCCM Flow rate through pinhole: 3 SLM Cell Pressure: 1 Torr	Cell C, OH yield Residence time: $\sim 60\,\mathrm{ms}$[3] Typical NO flow used during fieldwork: 100 SCCM Flow rate through pinhole: 3.5 SLM Cell Pressure: 1.5 Torr
Ethene	10	0.057 ± 0.033	0.463 ± 0.030	–
	20	0.073 ± 0.029	–	–
	30	0.098 ± 0.025	–	–
	40	0.157 ± 0.047	–	–
	50	0.172 ± 0.057	–	–
	100	–	–	0.947 ± 0.073
Methanol	50	0.756 ± 0.273	–	–
Isoprene	50	0.178 ± 0.075	–	0.849 ± 0.057
Propane	50	0.00 ± 0.053	0.00 ± 0.102	–
Methane	100	–	–	0.00 ± 0.091
Cyclohexane	100	–	–	0.606 ± 0.051
Toluene	100	–	–	0.874 ± 0.072

[1] Determined by computational fluid dynamics, for further details refer to Creasey et al. (1997b).

[2] Experiments during which the NO concentration was varied from 10–50 SCCM and compared to modelled OH yields (see Fig. 6) suggest that NO that mixes into to the air flow is actually 5.5 times less than the NO that is injected.

[3] Estimated from comparison of experimentally determined OH yield from ethane-derived RO_2 radicals and MCM-predicted yields (see Fig. 5).

Table 2. OH yields in time-resolved experiments from peroxy radicals determined using Eqs. (2) and (3); the MCMv3.2 OH yield is provided in the final columns for comparison. The modelled OH yield was determined using Eq. (4) calculated after 9.8 ms integration time. The model was constrained with a $[NO] = 1 \times 10^{14}$ molecule cm^{-3} and a temperature = 298 K (fourth column) or $[NO] = 1 \times 10^{14}$ molecule cm^{-3} and a temperature = 255 K (final column).

Source of peroxy radicals	OH yield (referenced to methanol)	OH Yield (referenced to ethene)	MCM OH yield (referenced to initial $[RO_2]$) at 298 K	MCM OH yield (referenced to initial $[RO_2]$) at 255 K
Methanol	1.00 ± 0.08	0.85 ± 0.09	1.00	–
Isoprene	1.03 ± 0.11	0.92 ± 0.04	0.90	–
Ethene	1.17 ± 0.09	1.00 ± 0.08	0.99	0.90
Cyclohexane	0.45 ± 0.09	0.38 ± 0.08	0.74	0.36
Propane	0.042 ± 0.008	0.034 ± 0.008	0.01	–
Propene	1.17 ± 0.13	–	–	–
n-butane	0.35 ± 0.04	0.18 ± 0.01	0.13 (0.12)	0.12
n-pentane	–	0.48 ± 0.01	0.62 (0.49)	0.49

Fig. 1. Schematics highlighting the key features of the three FAGE cells tested. Cell A was used for sequential OH and HO_2 detection during the OP3 project; dotted line highlights internal cell components. Cell B was used to make sequential tower-based measurements of OH and HO_2 during the HCCT campaign. Cell C represents the coupling of a reaction tube to a FAGE cell (cell A design) for detection of RO_2 radicals by LIF, see text for further details.
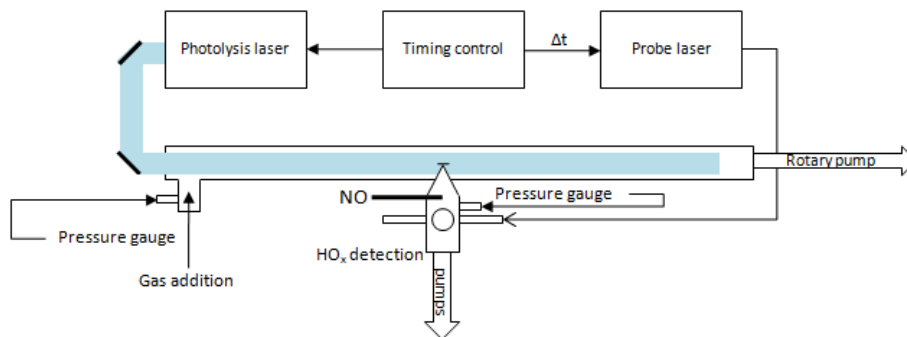
Fig. 2. Schematic highlighting the key features of the laser flash-photolysis time-resolved experimental set-up.
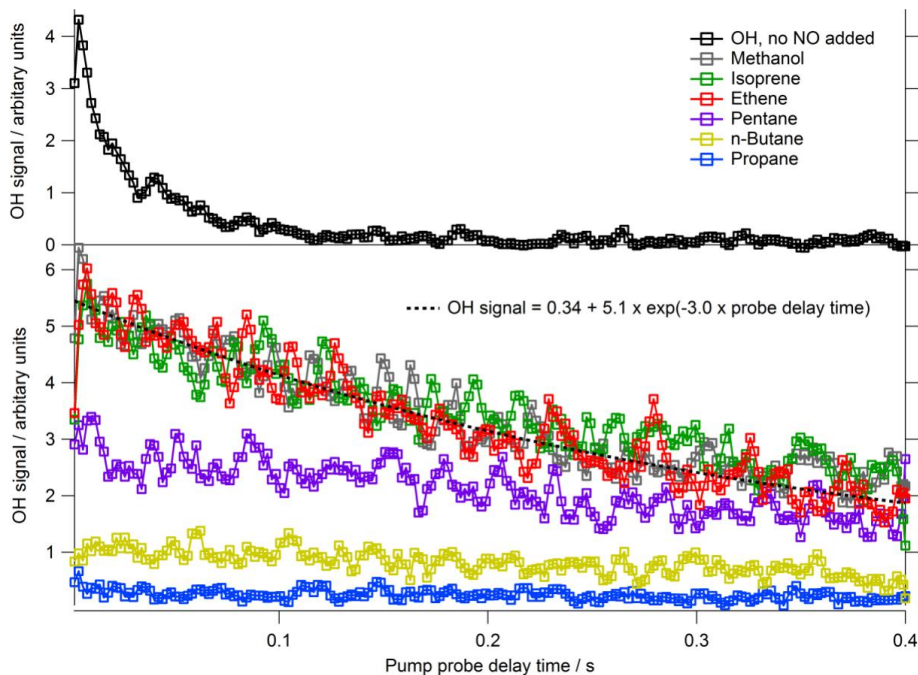
Fig. 3. upper panel: Time evolution of OH formed in the flow tube by laser-photolysis of O_3 in humidified air in the presence of isoprene with no NO added to the FAGE cell. Lower panel: Typical time-resolved experiments showing the OH signal from isoprene (green), ethene (red), methanol (grey), *n*-pentane (purple), *n*-butane (mustard) and propane (blue) derived peroxy radicals that was observed when 6 SCCM NO was added to the FAGE cell. The dashed line shows the fit to the OH signal from ethene-derived RO_2 radicals of the function: $y = y_0 + A \times \exp(-B \times x)$. The relative yields were determined from the ratio of the *A* factors. See Table 2 for the yields determined.
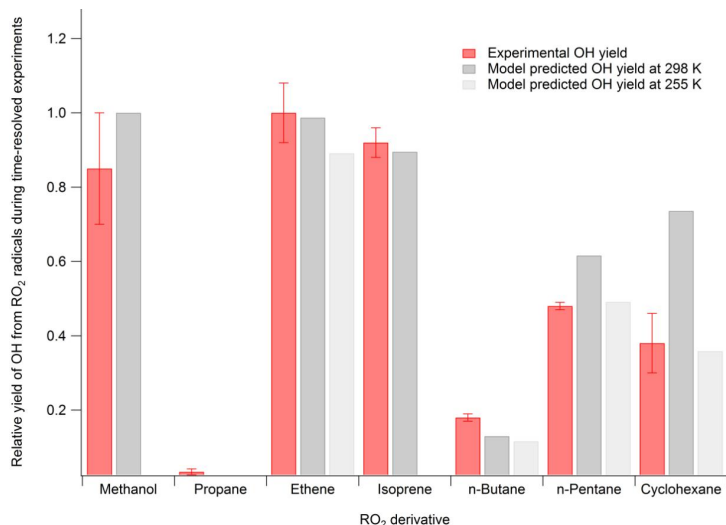
Fig. 4. Time-resolved OH yields (using apparatus outlined in Fig. 2) from different peroxy radicals ($RO_2 \rightarrow HO_2 \rightarrow OH$) under low-pressure FAGE conditions in the presence of NO (red bars); the errors represent the 1σ variability of the determined experimental yield. The Kintecus model predicted OH yields, assuming a reaction time of 9.8 ms and an initial NO concentration of 1×10^{14} molecule cm^{-3}, based on MCMv3.2 chemistry (model schemes provided in SI), assuming a temperature of 298 K (dark grey bars) are also shown for comparison. The model predicted OH yield at 255 K for ethene, *n*-butane, *n*-pentane and cyclohexane are represented by the light grey bars. The strong temperature dependence for the rate of isomerisation/decomposition of the alkoxy radicals reduces the model predicted OH yield as reaction between alkoxy radicals + NO Reaction (R19) begins to compete; there is currently no information on the temperature dependence of isoprene-derived alkoxy radical decomposition in the literature.

Discussion Paper | Discussion Paper | Discussion Paper | Discussion Paper

AMTD

6, 6249–6292, 2013

Sensitivity of Laser Induced Fluorescence instruments

L. K. Whalley et al.

Title Page

Abstract | Introduction

Conclusions | References

Tables | Figures

◄ | ►

◄ | ►

Back | Close

Full Screen / Esc

Printer-friendly Version

Interactive Discussion

Fig. 5. Upper panel: The OH yields from different peroxy radicals ($RO_2 \rightarrow HO_2 \rightarrow OH$) in cell A in the presence of NO (blue bars); the errors represent the 1σ variability of the determined experimental yield. The model predicted OH yields (grey bars) assuming a reaction time of 0.9 ms, temperature of 255 K and an initial NO concentration of 1×10^{14} molecule cm^{-3}, based on MCMv3.2 chemistry are also shown for comparison. Middle panel: The OH yields from different peroxy radicals ($RO_2 \rightarrow HO_2 \rightarrow OH$) in cell B in the presence of NO (purple bars); the errors represent the 1σ variability of the determined experimental yield. The model predicted OH yields (grey bars) assuming a reaction time of 1.9 ms, temperature of 255 K and an initial NO concentration of 1×10^{14} molecule cm^{-3}, based on MCMv3.2 chemistry are also shown for comparison. Lower panel: The OH yields from different peroxy radicals ($RO_2 \rightarrow HO_2 \rightarrow OH$) in cell C in the presence of NO (green bars); the errors represent the 1σ variability of the determined experimental yield. The model predicted OH yields (grey bars) assuming a reaction time of 60 ms, an initial NO concentration of 1×10^{13} molecule cm^{-3} and a temperature of 255 K based on MCMv3.2 chemistry are also shown for comparison; there is currently no information on the temperature dependence of isoprene- or toluene-derived alkoxy radical decomposition in the literature so the rate coefficient at 298 K is assumed.

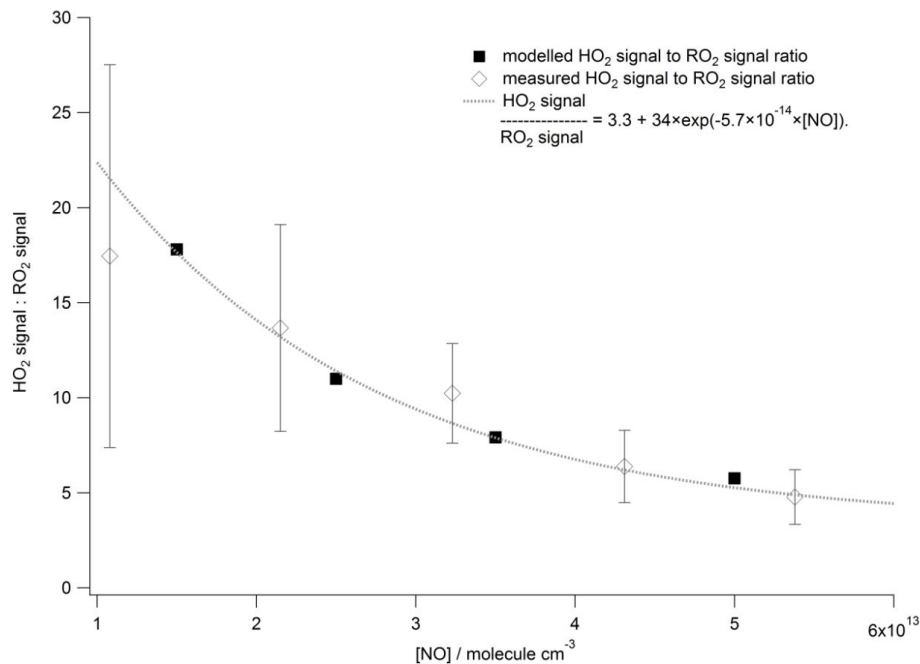**Fig. 6.** Modelled (filled squares) and measured (open diamonds) ratio of the OH yield from $HO_{2\ signal} : RO_{2\ signal}$ as a function of NO concentration. For best agreement with model predictions, it has to be assumed that the NO concentration that mixes into the ambient air stream is 5.5 times lower than the amount actually injected. The dashed line represents the line of best fit for the modelled HO_2 signal to RO_2 signal ratio as a function of NO. The error bars represent the fractional error associated with each measured ratio determined from the 1σ standard deviation of the experiments conducted.

Title Page

Abstract | Introduction

Conclusions | References

Tables | Figures

◄ | ►►|

◄ | ►

Back | Close

Full Screen / Esc

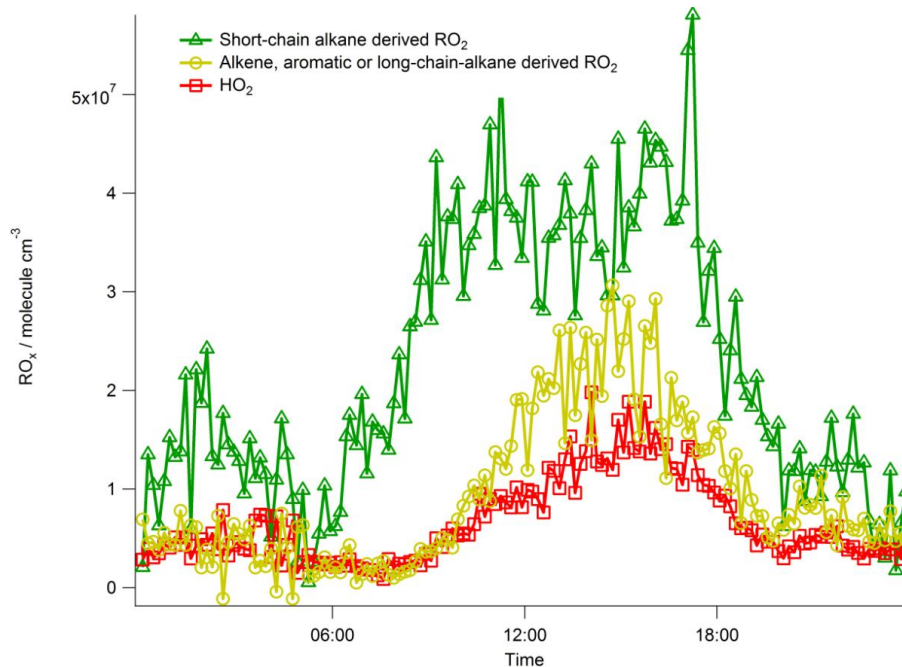Printer-friendly Version

Interactive Discussion

Fig. 7. Campaign average diurnals of short-chain alkane RO_2 radicals (green), HO_2 (red) and alkene or aromatic or long-chain alkane derived RO_2 radicals (mustard) from the ClearfLo project which took place in London (North Kensington) from the 21 July to 18 August 2012.